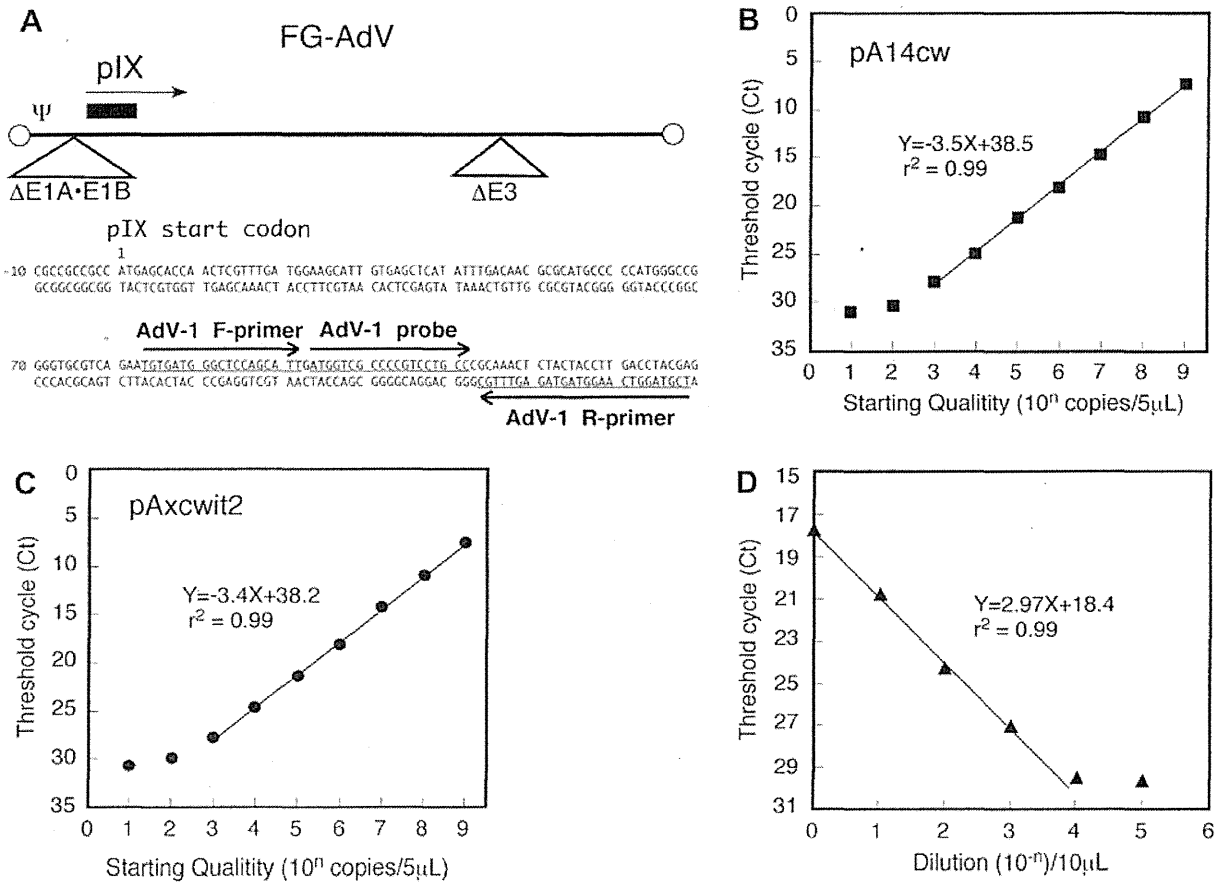

Fig. 2. (A) Position of the AdV-1 primers and the fluorogenic probe. The locations of the packaging signal (Ψ) and the coding region of the pIX gene are indicated. The arrows indicate the direction of transcription. AdV-1 F-primer, R-primer, and probe were designed using the program Primer Express 1.5 (Applied Biosystems), and their sequences are underlined. The primers and probes were selected according to the manufacturer's guidelines. The fluorogenic probes contained FAM (6-carboxylfluoroescein) at the 5′-end and TAMRA (6-carboxyltetramethylrhodamine) at the 3′-end. This set of primers/probe recognizes the coding region of the pIX gene. (B), (C), and (D) are the standard calibration curves for plasmids, cosmids and FG-AdV including the pIX gene, respectively. The standard calibration curves for the threshold cycle values (Ct) versus the copy number using serial dilutions of pA14cw (B) or pAxcwit2 (C) are shown. Similarly, serial dilutions of AxCAGFP vectors were used to generate the standard curve (D). The coefficients of correlation (r^2) are indicated.

of HeLa cells, respectively (column "GIT ratio", 0.3 for CV-1 and 0.06 for NIH-3T3), showing that GIT varied among different cell types.

However, because the control virus infected in parallel was identically influenced by the infection conditions, including the cell concentration and the cell type, the copy numbers of testing virus relative to that of the control virus can be calculated using the Ct value of the control virus as shown below. The relative GIT, called the rVT, is defined as follows:

$$\text{rVT} = (\text{control virus GIT}) \times 2^{(\text{control viral Ct} - \text{testing viral Ct})}(/\text{mL})$$

(Note that, because one *lower* Ct value means 2-fold *more* DNA, "$2^{(\text{testing viral Ct} - \text{control viral Ct})}$" is not correct).

For example, if control virus GIT, control viral Ct and testing viral Ct are 2.4×10^8 (copies/mL), 22.6 and 19.4, respectively, in a particular titration using CV-1 cells, the $\text{rVT} = 2.4 \times 10^8 \times 2^{(22.6-19.4)} = 2.4 \times 10^8 \times 2^{3.2} = 2.2 \times 10^9$ (copies/mL).

Because the rVTs of CV-1 and HeLa cells at the concentrations of 6.0×10^5 cells per well (full-sheet condition) were similar, i.e., 2.3×10^9 (copies/mL), the rVT calculated using the data of Fig. 2D can be applied to the rVT of HeLa cells. The rVTs measured using HeLa cell concentrations of 0.6×10^5, 2.0×10^5 and 6.0×10^5 cells per well were 0.9×10^9, 1.0×10^9 and 2.3×10^9 copies/μL, respectively (Table 1, rVT/mL): the ratio of rVTs obtained using three different cell concentrations (column "rVT ratio") was 0.4:0.4:1. Similar experiments using CV-1 cells indicated that the ratio was 1.2:1.2:1, showing that the rVT was less influenced by the cell concentration than the GIT. Table 1 also showed that, though the GIT of NIH-3T3 was extremely different from that of HeLa and CV-1, the rVT of NIH-3T3 was very similar to those of CV-1 and HeLa (column of "rVT ratio"). Therefore, even using different cell lines and dilutions, the rVT did not fluctuate, indicating that about the same rVT can be obtained using various types of cells other than HeLa cells for the purpose of titration. Because HeLa cells are commonly used worldwide, we recommend the use of HeLa cells for rVT measurements. Importantly, the present results also showed that the

Table 1
Differences between GIT and rVT among various cell concentration and cell lines.

Cells	No. of cells $\times 10^5$	GIT Copies/mL $\times 10^9$	GIT Ratio	rVT rVT/mL $\times 10^9$	rVT Ratio
HeLa	0.6	137.8 ± 6.4	4.9	0.9 ± 0.4	0.4
	2.0	89.5 ± 2.0	3.2	1.0 ± 0.2	0.4
	6.0	28.2 ± 1.8	1	2.3 ± 0.1	1
CV-1	6.0	8.2 ± 1.7	0.3	2.3 ± 0.1	1.0
NIH3T3 6.0	6.0	1.7 ± 0.3	0.06	1.0 ± 0.4	0.4

Two independent experiments were performed using the virus dilutions of 10^1 and 10^2.

Table 2
Infection conditions.

Condition	GIT/mL ($\times 10^9$)	Ratio
Plate	0.8 ± 0.3	1
Suspension	0.8 ± 0.2	1.0

The presentations are the same as Table 1.

Table 3
Days after infections.

Day	GIT/mL ($\times 10^9$)	Ratio
1	2.5 ± 0.1	1.6
2	1.6 ± 0.1	1
3	1.6 ± 0.4	1.0

The presentations are the same as Table 1.

rVT can be compared even when different cell lines or amounts of AdV were used.

The quality of the control virus does not significantly influence on the rVT value as far as the same lot of the control virus is used. Therefore, a conventional virus can be used as the control virus without purification. If strict comparison between the rVTs measured in different laboratories is needed, the adenovirus type 5 reference material may be useful and is available from ATCC (VR-1516) [23]. If a gene product of the testing virus is extremely deleterious to the target cells, the infected cells possibly grow slowly and the ratio of the copy number of the viral genome against that of β-actin on the cell chromosome may increase. However, if this is the case, the obtained rVT values of 10^{-1} dilution (high dose) and 10^{-2} dilution (low dose) must differ significantly, because the latter should be less influenced than the former. We have not experienced these cases.

3.4. Examination of infection conditions

We also examined whether the transduction efficiency of AdV differs when the cells to be infected are attached to a plate (plating method) or present in suspension (suspension method). In the former method, a monolayer of cells on the plate was incubated with an aliquot of AxCAGFP stock for 1 h for 37 °C, with shaking every 15 min before adding the medium. In the latter method, cells detached by trypsin were mixed with the virus, incubated for 5 min at room temperature, mixed with medium, and transferred to a 6-well or 24-well plate. The results showed no significant differences between the two methods for two different virus dilutions (Table 2). Because the suspension method is very simple and quick, we used the suspension method thereafter. Next, we examined the detected copy numbers of the transduced viral genome on days 1, 2 and 3. After washing the cells with PBS (−) on each day, the total infected-cell DNA was extracted, and the amounts of AdV genome were measured using qPCR (Table 3). The detected AdV copy number on day 1 was higher than that on day 2, but those on day 2 and day 3 were equal, suggesting that the number had reached a plateau level. The results were consistent with those for the Southern blot experiments (Fig. 1B, 48 h and 72 h). Consequently, we adopted day 2 for the measurement of rVT. Therefore, for the rVT method the infection protocol is very simple, and titration results can be obtained in only 2 days. The use of the infection protocol is not limited to AdV titration, but can also be used for ordinary AdV infection experiments. The rVT protocol is described in Supplementary Information.

3.5. Examples where the $TCID_{50}$ titer differed from the rVT

The ratio of the rVT value and the authentic $TCID_{50}$ titer were well correlated. AxEFLNLG is one example of an FG AdV; this AdV expresses neo protein unless the neo gene flanked by a pair of *lox*Ps is excised during Cre-mediated recombination. Because the neo gene is popularly used to establish neo-resistant cell lines, it must not be toxic. The rVT/mL and $TCID_{50}$/mL of a viral stock of this AdV were measured using CV-1 cells as a target and 293 cells, in which AdV proliferates, respectively. As shown in Table 4, in the first line, the ratio of rVT/$TCID_{50}$ was 0.3 using CV-1 for rVT; if HeLa cells are used for the rVT, the ratio should be $0.3 \times 0.6 \approx 0.2$ based on the data in Table 1. Thus, the $TCID_{50}$/mL was normally five times higher than the rVT/mL value when using HeLa as the target cells. Therefore, the ratio is normally useful when converting the values from one to another.

Table 4
Differences between rVT and $TCID_{50}$.

AdVs	rVT/mL	$TCID_{50}$/mL	rVT/$TCID_{50}$	Ratio
AxEFLNLG	$0.4 \pm 0.1 \times 10^9$	$1.8 \pm 0.2 \pm 10^9$	0.2	1
AxEFdsRed	$2.3 \pm 0.1 \times 10^9$	$0.3 \pm 0.1 \pm 10^9$	7.7	34.5
AxCANCre	$2.6 \pm 0.4 \times 10^7$	$3.1 \pm 0.9 \pm 10^7$	0.8	3.8

The presentations are the same as Table 1.

However, the ratio sometimes differed; for AxEFdsRed, an AdV that highly expresses dsRed protein, the copy number transduced to the target cells obtained using rVT was 18-times higher than that obtained using the $TCID_{50}$ method. AxCANCre, which highly expresses Cre recombinase, also produced an rVT value that was 3.3-times higher than that obtained using the $TCID_{50}$ method. Because the rVT value reflects the copy numbers in transduced target cells that are important for expression experiments, it is more valuable than the $TCID_{50}$ titer. Also, the rVT method can be applied for the titration of viruses that cannot proliferate in 293 cells, such as HD-AdV and other DNA and RNA viral vectors that do not replicate in the target cells.

In summary, we used Cre recombination and showed that the majority of the AdV genome detected in infected cells indicated successfully transduced molecules and that qPCR can certainly be used for AdV titration. Although cell concentrations and cell types influence the GIT tremendously, these factors can be corrected using a "control AdV" in parallel; hence, we established the rVT method, which can be used to determine the amount of actively infectious AdV genome present in the target cells. This method is quick, reliable, and superior to current titration methods using 293 cells.

Acknowledgments

The authors thank Ms. M. Terashima and Mr. Y. Ohno for technical support. Funding for this research was provided by a Grant in Aid for Scientific Research on Priority Areas from Ministry of Education, Culture, Sports, Science and Technology, Japan (to I.S.).

Appendix A. Supplementary data

Supplementary data associated with this article can be found, in the online version, at doi:10.1016/j.bbrc.2011.12.016.

References

[1] S. Kondo, Y. Takata, M. Nakano, I. Saito, Y. Kanegae, Activities of various FLP recombinases expressed by adenovirus vectors in mammalian cells, J. Mol. Biol. 390 (2009) 221–230.

[2] F.L. Graham, A.J. van der Eb, A new technique for the assay of infectivity of human adenovirus 5 DNA, Virology 52 (1973) 456–467.

[3] B. Precious, W.C. Russell, Growth, purification and titration of adenovirus, in: B.M. Mahy (Ed.), Virology: A Practical Approach, IRL Press, Oxford, 1985, pp. 193–205.
[4] Y. Kanegae, M. Makimura, I. Saito, A simple and efficient method for purification of infectious recombinant adenovirus, Jpn. J. Med. Sci. Biol. 47 (1994) 157–166.
[5] R. Mentel, E. Matthes, M. Janta-Lipinski, U. Wegner, Fluorescent focus reduction assay for the screening of antiadenoviral agents, J. Virol. Methods 59 (1996) 99–104.
[6] L. Philipson, Adenovirus assay by the fluorescent cell-counting procedure, Virology 15 (1961) 263–268.
[7] B. Bewig, W.E. Schmidt, Accelerated titering of adenoviruses, Biotechniques 28 (2000) 870–873.
[8] N. Mittereder, K.L. March, B.C. Trapnell, Evaluation of the concentration and bioactivity of adenovirus vectors for gene therapy, J. Virol. 70 (1996) 7498–7509.
[9] L. Ma, H.A. Bluyssen, M. De Raeymaeker, V. Laurysens, N. van der Beek, H. Pavliska, A.J. van Zonneveld, P. Tomme, H.H. van Es, Rapid determination of adenoviral vector titers by quantitative real-time PCR, J. Virol. Methods 93 (2001) 181–188.
[10] J. Crettaz, C. Olague, A. Vales, I. Aurrekoetxea, P. Berraondo, I. Otano, S. Kochanek, J. Prieto, G. Gonzalez-Aseguinolaza, Characterization of high-capacity adenovirus production by the quantitative real-time polymerase chain reaction: a comparative study of different titration methods, J. Gene Med. 10 (2008) 1092–1101.
[11] M. Puntel, J.F. Curtin, J.M. Zirger, A.K. Muhammad, W. Xiong, C. Liu, J. Hu, K.M. Kroeger, P. Czer, S. Sciascia, S. Mondkar, P.R. Lowenstein, M.G. Castro, Quantification of high-capacity helper-dependent adenoviral vector genomes in vitro and in vivo, using quantitative TaqMan real-time polymerase chain reaction, Hum. Gene Ther. 17 (2006) 531–544.
[12] F. Kreppel, V. Biermann, S. Kochanek, G. Schiedner, A DNA-based method to assay total and infectious particle contents and helper virus contamination in high-capacity adenoviral vector preparations, Hum. Gene Ther. 13 (2002) 1151–1156.
[13] V. Sandig, R. Youil, A.J. Bett, L.L. Franlin, M. Oshima, D. Maione, F. Wang, M.L. Metzker, R. Savino, C.T. Caskey, Optimization of the helper-dependent adenovirus system for production and potency in vivo, Proc. Natl. Acad. Sci. USA 97 (2000) 1002–1007.
[14] F.L. Graham, J. Smiley, W.C. Russell, R. Nairn, Characteristics of a human cell line transformed by DNA from human adenovirus type 5, J. Gen. Virol. 36 (1977) 59–74.
[15] Y. Kanegae, G. Lee, Y. Sato, M. Tanaka, M. Nakai, T. Sakaki, S. Sugano, I. Saito, Efficient gene activation in mammalian cells by using recombinant adenovirus expressing site-specific Cre recombinase, Nucleic Acids Res. 23 (1995) 3816–3821.
[16] Y. Kanegae, M. Terashima, S. Kondo, H. Fukuda, A. Maekawa, Z. Pei, I. Saito, High-level expression by tissue/cancer-specific promoter with strict specificity using a single-adenoviral vector, Nucleic Acids Res. 39 (2010) e7.
[17] S. Miyake, M. Makimura, Y. Kanegae, S. Harada, Y. Sato, K. Takamori, C. Tokuda, I. Saito, Efficient generation of recombinant adenoviruses using adenovirus DNA-terminal protein complex and a cosmid bearing the full-length virus genome, Proc. Natl. Acad. Sci. USA 93 (1996) 1320–1324.
[18] I. Saito, Y. Oya, K. Yamamoto, T. Yuasa, H. Shimojo, Construction of nondefective adenovirus type 5 bearing a 2.8-kilobase hepatitis B virus DNA near the right end of its genome, J. Virol. 54 (1985) 711–719.
[19] I. Saito, R. Groves, E. Giulotto, M. Rolfe, G.R. Stark, Evolution and stability of chromosomal DNA coamplified with the CAD gene, Mol. Cell Biol. 9 (1989) 2445–2452.
[20] J. Sambrook, D.W. Russell, Molecular Cloning, third ed., Cold Spring Harbor Laboratory Press, New York, 2001.
[21] M. Nakano, K. Odaka, Y. Takahashi, M. Ishimura, I. Saito, Y. Kanegae, Production of viral vectors using recombinase-mediated cassette exchange, Nucleic Acids Res. 33 (2005) e76.
[22] H. Fukuda, M. Terashima, M. Koshikawa, Y. Kanegae, I. Saito, Possible mechanism of adenovirus generation from a cloned viral genome tagged with nucleotides at its ends, Microbiol. Immunol. 50 (2006) 643–654.
[23] B. Huchins, N. Sajjadi, S. Seaver, A. Shepherd, S.R. Bauer, S. Simek, K. Carson, E. Aguilar-Cordova, Working toward an adenoviral vector testing standard, Mol. Ther. 2 (2000) 532–534.

HEPATOLOGY
Official Journal of the American Association for the Study of Liver Diseases

MicroRNA-140 Acts as a Liver Tumor Suppressor by Controlling NF-κB Activity by Directly Targeting DNa Methyltransferase 1 (Dnmt1) Expression

Akemi Takata,[1] Motoyuki Otsuka,[1] Takeshi Yoshikawa,[1] Takahiro Kishikawa,[1] Yohko Hikiba,[2] Shuntaro Obi,[3] Tadashi Goto,[1] Young Jun Kang,[4] Shin Maeda,[1] Haruhiko Yoshida,[1] Masao Omata,[1] Hiroshi Asahara,[5,6,7] and Kazuhiko Koike[1]

MicroRNAs (miRNAs) are small RNAs that regulate the expression of specific target genes. While deregulated miRNA expression levels have been detected in many tumors, whether miRNA functional impairment is also involved in carcinogenesis remains unknown. We investigated whether deregulation of miRNA machinery components and subsequent functional impairment of miRNAs are involved in hepatocarcinogenesis. Among miRNA-containing ribonucleoprotein complex components, reduced expression of DDX20 was frequently observed in human hepatocellular carcinomas, in which enhanced nuclear factor-κB (NF-κB) activity is believed to be closely linked to carcinogenesis. Because DDX20 normally suppresses NF-κB activity by preferentially regulating the function of the NF-κB-suppressing miRNA-140, we hypothesized that impairment of miRNA-140 function may be involved in hepatocarcinogenesis. DNA methyltransferase 1 (Dnmt1) was identified as a direct target of miRNA-140, and increased Dnmt1 expression in DDX20-deficient cells hypermethylated the promoters of metallothionein genes, resulting in decreased metallothionein expression leading to enhanced NF-κB activity. MiRNA-140-knockout mice were prone to hepatocarcinogenesis and had a phenotype similar to that of DDX20 deficiency, suggesting that miRNA-140 plays a central role in DDX20 deficiency-related pathogenesis. ***Conclusion*****: These results indicate that miRNA-140 acts as a liver tumor suppressor, and that impairment of miRNA-140 function due to a deficiency of DDX20, a miRNA machinery component, could lead to hepatocarcinogenesis.** (HEPATOLOGY 2013;57:162-170)

Hepatocellular carcinoma (HCC) is the third most common cause of cancer-related mortality worldwide.[1] Although multiple major risk factors have been identified, such as infection with hepatitis viruses B or C, the molecular mechanisms underlying HCC development remain poorly understood, hindering the development of novel therapeutic approaches. Therefore, a better understanding of the molecular pathways involved in hepatocarcinogenesis is critical for the development of new therapeutic options.

Nuclear factor-κB (NF-κB) is one of the best-characterized intracellular signaling pathways. Its activation is a common feature of human HCC.[2-4] It acts as an inhibitor of apoptosis and as a tumor promoter[4,5] and is associated with the acquisition of a transformed phenotype during hepatocarcinogenesis.[6] In fact, studies using patient samples suggest that NF-κB activation in the liver leads to the development of HCC.[7] Although there are conflicting reports,[8] activation of the NF-κB pathway in the liver is crucial for the initiation and promotion of HCC.[4]

Abbreviations: DEN, diethylnitrosamine; Dnmt1, DNA methyltransfemse 1; HCC, hepatocellular carcinoma; miRNA; microRNA; miRNP, miRNA-containing ribonucleoprotein; MT, metallothionein; NF-κB, nuclear factor-κB; RT-PCR, reverse-transcription polymerase chain reaction; TNF-α, tumor necrosis factor-α; TRAIL, TNF-related apoptosis-inducing ligand; UTR, untranslated region.

From the [1]Department of Gastroenterology, Graduate School of Medicine, The University of Tokyo, Tokyo, Japan; the [2]Division of Gastroenterology, Institute for Adult Diseases, Asahi Life Foundation, Tokyo, Japan; the [3]Department of Hepatology, Kyoundo Hospital, Tokyo, Japan; the [4]Department of Immunology and Microbial Science, and the [5]Department of Molecular and Experimental Medicine, The Scripps Research Institute, La Jolla, CA; the [6]Department of Systems BioMedicine, Tokyo Medical and Dental University, Tokyo, Japan; and [7]CREST, Japan Science and Technology Agency, Tokyo, Japan.

Received March 30, 2012; accepted July 18, 2012.

Supported by Grants-in-Aid from the Ministry of Education, Culture, Sports, Science and Technology, Japan (#22390058, #23590960, and #20390204) (M. O., T. G., and K. K.); Health Sciences Research Grants from the Ministry of Health, Labor and Welfare of Japan (Research on Hepatitis) (to K. K.); National Institutes of Health Grant R01AI088229 (to Y. J. K.); the Miyakawa Memorial Research Foundation (to A. T.); and grants from the Sagawa Foundation for Promotion of Cancer Research, the Astellas Foundation for Research on Metabolic Disorders, and the Cell Science Research Foundation (to M. O.).

MicroRNAs (miRNAs) are small RNA molecules that regulate the expression of target genes and are involved in various biological functions.[9-12] Although specific miRNAs can function as either suppressors or oncogenes in tumor development, a general reduction in miRNA expression is commonly observed in human cancers.[13-22] In this context, it can be hypothesized that deregulation of the machinery components involved in miRNA function may be related to the functional impairment of miRNAs and the pathogenesis of carcinogenesis.

In this study, we show that the expression of DDX20, an miRNA-containing ribonucleoprotein (miRNP) component, is frequently decreased in human HCC. Because DDX20 is required for both the preferential loading of miRNA-140 into the RNA-induced silencing complex and its function,[23] we hypothesized that DDX20 deficiency would lead to hepatocarcinogenesis via impaired miRNA-140 function. MiRNA-140 knockout mice were indeed more prone to hepatocarcinogenesis, and we identified a possible molecular pathway from DDX20 deficiency to liver cancer.

Materials and Methods

Mouse and Liver Tumor Induction. MiRNA-140$^{-/-}$ mice have been described.[24] Recombinant murine tumor necrosis factor-α (TNF-α) (25 μg/kg; Wako, Osaka, Japan) was injected into the tail vein, and the mice were sacrificed 1 hour later. To induce liver tumors, 15-day-old mice received an intraperitoneal injection of diethylnitrosamine (DEN) (25 mg/kg body weight), and were sacrificed 32 weeks later. All animal experiments were performed in compliance with the regulations of the Animal Use Committee of the University of Tokyo and the Institute for Adult Disease, Asahi Life Foundation.

Plasmids. FLAG-tagged human DDX20-expressing plasmids were as described.[23] The pGL3-based reporter plasmid containing Dnmt1 3′ untranslated region (UTR) sequences was provided by G. Marucucci.[25]

Detailed Materials and Methods. The detailed experimental procedures of clinical samples, cells, plasmids, reporter assays, reverse-transcription polymerase chain reaction (RT-PCR) analysis, antibodies, western blotting, cell assays, immunohistochemistry, microarray analysis, methylation analysis, and electrophoretic mobility-shift assay are described in the Supporting Information.

Statistical Analysis. Statistically significant differences between groups were determined using a Wilcoxon rank-sum test. A Wilcoxon signed-rank test was used for statistical comparisons of protein expression levels between HCC and surrounding noncancerous tissues.

Table 1. Cases with Differential Expression Levels of miRNP Components in HCC (n = 10)

Gene ID	Gene Symbol	Decreased	Increased	No Change
23405	Dicer1	2	1	7
27161	EIF2C2 (AGO2)	1	1	8
6895	TARBP2(TRBP2)	2	0	8
11218	DDX20 (GEMIN3)	8	0	2
50628	GEMIN4	1	0	9

The expression levels of each miRNP component were determined via immunohistochemistry.

The numbers indicate the number of cases that had the differential expression levels (decreased, increased, or no change) in HCC tissues compared with those in surrounding liver tissues.

Results

DDX20 Expression Is Frequently Decreased in HCC. The expression levels of proteins reported to be miRNP components (Dicer, Ago2, TRBP2, DDX20 [also known as Gemin3], and Gemin4)[26] were initially determined via immunohistochemistry in HCC and noncancerous background liver tissues from 10 patients. DDX20 expression was lower in HCC tissue compared with the surrounding noncancerous tissue in 8 of 10 cases, whereas expression of the other genes was unchanged (Table 1 and Supporting Fig. 1). Therefore, and because DDX20 was recently identified as a possible liver tumor suppressor in mice,[27] we determined its role as a human HCC suppressor.

DDX20 protein expression was lower in several HCC cell lines, such as Huh7 and Hep3B (Fig. 1A), compared with normal hepatocytes. DDX20 protein levels were also lower in human HCC needle biopsy specimens than in surrounding noncancerous liver tissue (Fig. 1B). Immunohistochemical analysis

Address reprint requests to: Motoyuki Otsuka, M.D., Department of Gastroenterology, Graduate School of Medicine, University of Tokyo, 7-3-1 Hongo, Bunkyo-ku, Tokyo 113-8655, Japan. E-mail: otsukamo-tky@umin.ac.jp; fax: (81)-3-3814-0021.

View this article online at wileyonlinelibrary.com.

DOI 10.1002/hep.26011

Potential conflict of interest: Nothing to report.

Additional Supporting Information may be found in the online version of this article.

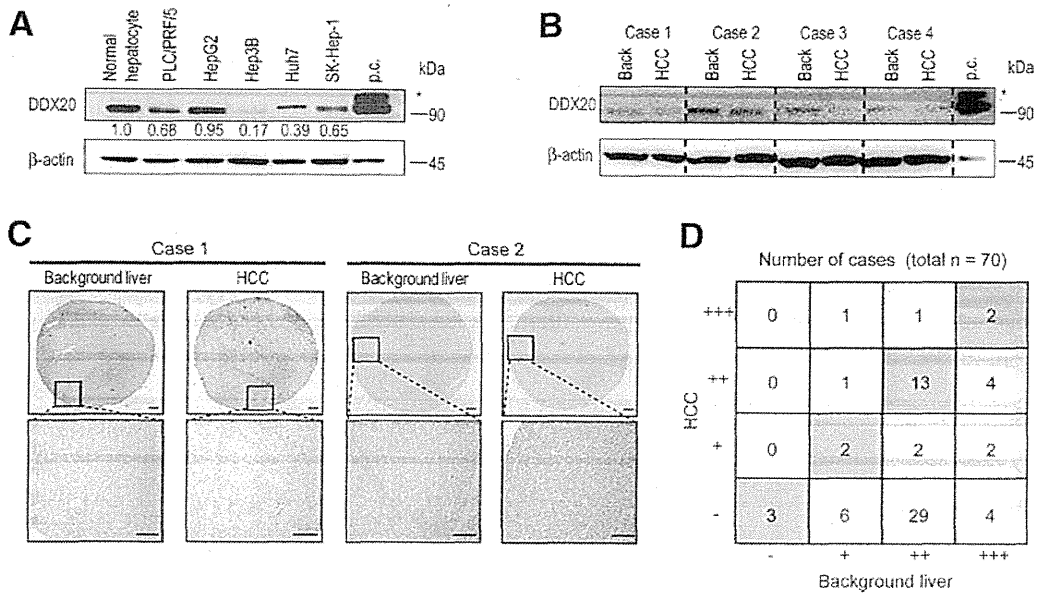

Fig. 1. Reduced DDX20 expression levels in hepatocellular carcinoma. (A) DDX20 protein expression in HCC cell lines. Numbers between the panels indicate DDX20 protein levels normalized to β-actin levels. Lysates of 293T cells transiently transfected with a FLAG-tagged DDX20-expressing plasmid yielded two DDX20 bands corresponding to the endogenous DDX20 protein and the transfected FLAG-tagged DDX20 protein (*) as a positive control (p.c.; far right lane). Data represent the results of three independent determinations. (B) DDX20 protein expression in four HCC needle biopsy specimens and in the surrounding noncancerous background liver tissue (Back). *Positive control. (C) Immunohistochemical analysis of DDX20 protein expression in HCC and surrounding tissues (background liver). Two representative cases are shown. Scale bars, 500 μm. The lower panels display magnified images of the boxed areas in the upper panels. (D) Grid summarizing DDX20 immunohistochemical staining data from 70 cases. In 47 cases (pink shading), DDX20 protein levels were lower in the HCC tissues than in the surrounding tissues ($P < 0.05$; Wilcoxon signed-rank test).

confirmed that DDX20 expression was frequently lower in HCC than in surrounding noncancerous liver tissue (Fig. 1C,D). Specifically, 47 of 70 cases examined showed reduced DDX20 protein expression in HCC versus background noncancerous liver tissue (Fig. 1D and Supporting Table 1). These results indicate that the expression of DDX20, an miRNP component, is frequently reduced in human HCC, and suggest that this reduced DDX20 expression might be involved in the pathogenesis of a subset of HCC cases.

NF-κB Activity Is Enhanced by DDX20 Deficiency. Because DDX20 knockout mice are embryonic-lethal,[28] DDX20 has been suggested to have important biological roles. DDX20, a DEAD-box protein,[29] was originally found to interact with survival motor neuron protein.[30] Later, it was identified as a major component of miRNPs,[31] which may mediate miRNA function. As we have reported, DDX20 is preferentially involved in miRNA-140-3p function,[23] acting as a suppressor of NF-κB activity in the liver.[32] DDX20-knockdown PLC/PRF/5 cells exhibit enhanced NF-κB activity[23] (Fig. 2A). Whereas the proliferation rates of DDX20-knockdown cells and control cells were comparable (Fig. 2B), apoptotic cell death after stimulation with TNF-related apoptosis-inducing ligand (TRAIL), which induces both cell apoptosis and NF-κB activation,[33] was significantly reduced in DDX20-knockdown cells (Fig. 2C). Similar results were obtained using DDX20-knockdown HepG2 cells (Supporting Fig. 2A-D). Conversely, NF-κB activity was reduced, but cell proliferation remained unchanged, in Hep3B cells stably overexpressing DDX20 (Fig. 2D,E). Sensitivity to TRAIL-induced apoptosis was restored in these cells (Fig. 2F). Similar results were also obtained using Huh7 cells (Supporting Fig. 2E-H). These data confirm a previous report that DDX20 deficiency enhances NF-κB activity and the downstream events of this pathway.

Metallothionein Expression Is Decreased by DDX20 Deficiency. Next, to investigate the biological consequences of DDX20 deficiency, we examined the changes in transcript levels in DDX20-knockdown cells using microarrays (GEO accession number: GSE28088). The expression of genes driven by NF-κB that are related to carcinogenesis, such as FASLG, IRAK1, CARD9, and Galectin-1, were enhanced significantly in DDX20-knockdown cells, as expected (Table 2). To determine the mechanism underlying the enhanced NF-κB activation in DDX20-deficient cells, we searched for candidate genes and noticed that the

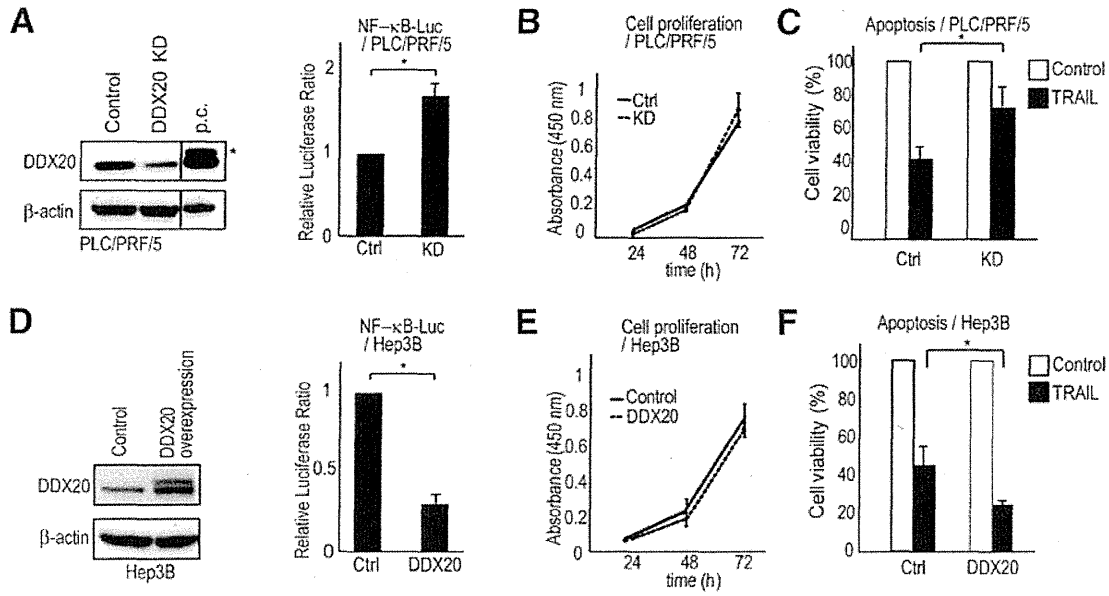

Fig. 2. Modulation of downstream events of the nuclear factor-κB pathway by DDX20. (A) Left: Establishment of stable DDX20-knockdown (DDX20 KD) PLC/PRF/5 cells. *Positive control (p.c.). Right: DDX20 deficiency enhances TNF-α–induced NF-κB activity. NF-κB reporter plasmids were transiently transfected into control (Ctrl) or DDX20-knockdown (KD) PLC/PRF/5 cells. The cells were then treated with TNF-α (5 ng/mL) or vehicle for 6 hours. $*P < 0.05$. Data are presented as the mean ± SD of three independent determinations. (B) Cell proliferation rates were comparable for control (Ctrl) and DDX20-knockdown (KD) PLC/PRF/5 cells. Data are presented as the mean ± SD of three determinations. (C) DDX20 deficiency reduces TRAIL-induced apoptotic cell death. Control (Ctrl) and DDX20-knockdown (KD) PLC/PRF/5 cells were incubated with 25 ng/mL TRAIL. Data represent cell viability after TRAIL stimulation (gray bars) relative to the number of vehicle-treated cells (white bars). $*P < 0.05$. Data are presented as the mean ± SD of triplicate determinations. (D) Left: Establishment of stable DDX20-overexpressing cells. Hep3B cells were infected with control or FLAG-tagged DDX20-overexpressing lentiviruses and selected on puromycin. Western blot analysis confirmed increased expression of DDX20 protein. Right: DDX20 overexpression suppresses TNF-α–induced NF-κB activity. NF-κB reporter plasmids were transiently transfected into Hep3B control (Ctrl) and DDX20-overexpressing (DDX20) cells treated with TNF-α for 6 hours. Data are presented as the mean ± SD of three independent determinations. $*P < 0.05$. (E) Proliferation of control (Ctrl) and DDX20-overexpressing (DDX20) Hep3B cells was measured as described in (B). (F) DDX20 overexpression reduces TRAIL-induced apoptotic cell death. Data for control (Ctrl) and DDX20-overexpressing (DDX20) Hep3B cells are shown. $*P < 0.05$.

Table 2. Increased Expression of NF-κB–Related Genes in DDX20-Knockdown HepG2 Cells Compared with Wild-Type Cells

RefSeq ID	Symbol	Description	Ratio	Representative Gene Function
NM_000639	FASLG	Fas ligand	3.5	NF-κB target, apoptosis
NM_052813	C9orf151	CARD9	2.5	NF-κB cascade, NF-κB target
NM_014959	CARD8	Tumor up-regulated CARD-containing antagonist of CASP9 (TUCAN)	2.2	NF-κB target
NM_131917	FAF1	FAS-associated factor 1 (hFAF1)	1.9	Cytoplasmic sequestering of NF-κB, NF-κB target
NM_020644	TMEM9B	Transmembrane protein 9B precursor	1.9	Positive regulation of NF-κB transcription factor activity
NM_017544	NKRF	ITBA4 protein	1.9	Negative regulation of transcription
NM_006247	PPP5C	Protein phosphatase T	1.8	Positive regulation of NF-κB cascade
NM_020345	NKIRAS1	KappaB-Ras1	1.8	NF-κB cascade
NM_001569	IRAK1	IRAK-1	1.7	Positive regulation of NF-κB transcription factor activity
NM_177951	PPM1A	Protein phosphatase 1A	1.7	Positive regulation of NF-κB cascade
NM_018098	ECT2	Epithelial cell-transforming sequence 2 oncogene	1.6	Positive regulation of NF-κB cascade
NM_002305	LGALS1	Galectin-1 (putative MAPK-activating protein MP12)	1.6	Positive regulation of NF-κB cascade
NM_015093	TAB2	TAK1-binding protein 2	1.6	Positive regulation of NF-κB cascade
NM_004180	TANK	TRAF-interacting protein	1.5	NF-κB cascade
NM_014976	PDCD11	Programmed cell death protein 11	1.5	rRNA processing
NM_015336	ZDHHC17	Putative NF-κB–activating protein 205	1.5	Positive regulation of NF-κB cascade
NM_002503	NFKBIB	IKB-β	1.5	Cytoplasmic sequestering of NF-κB
NM_138330	ZNF675	Zinc finger protein 675	1.5	Negative regulation of NF-κB transcription factor activity

The genes were identified as NF-κB–related based on the Gene Ontology and the GeneCodis Databases.

Table 3. Decreased Expression Levels of MT Genes in DDX20 Knockdown HepG2 Cells Compared with Wild-Type Cells

Symbol	Description	Ratio
MT1E	Metallothionein-1E	**0.12**
MT1F	Metallothionein-1F	**0.36**
MT1H	Metallothionein-1H	**0.16**
MT1G	Metallothionein-1G	**0.06**
MT1M	Metallothionein-1M	**0.24**
MT1X	Metallothionein-1X	**0.27**
MT2A	Metallothionein-2	**0.28**
MT3	Metallothionein-3	0.84
MTL5	Metallothionein-like 5 (Tesmin)	1.12

Numbers in boldface type indicate values <0.5.

expression levels of a group of metallothioneins (MTs), such as MT1E, MT1F, MT1G, MT1M, MT1X, and MT2A, were all significantly decreased when DDX20 was deficient (Table 3). The decreased expression of MTs in DDX20-knockdown HepG2 and PLC/PRF/5 cells was confirmed via quantitative RT-PCR (Fig. 3a and Supporting Fig. 3). Expression of MT-3, which was not altered in the microarray analysis, was similarly unaltered in quantitative RT-PCR analysis. Notably, it was already known that MTs are frequently silenced in human primary liver cancers.[34-36] In addition, MT knockout mice have enhanced NF-κB activity, likely due to reactive oxygen species, and these mice are more prone to hepatocarcinogenesis.[37] These results suggest that DDX20 deficiency enhances NF-κB activity by decreasing the expression of MTs, which could facilitate the development of liver cancer.

MiRNA-140 Directly Targets Dnmt1. Because MT expression is regulated principally by CpG island methylation in their promoter regions,[38,39] we examined the quantitative methylation status of MT promoters in DDX20-knockdown cells. The CpG islands of the MT1E, MT1G, MT1M, MT1X, and MT2A promoters, and the CpG shores of the MT1F promoters, were significantly more highly methylated under DDX20-deficient conditions, as determined by the comprehensive Illumina Quantitative Methylation BeadChip method (Table 4, Supporting Table 2, and GSE 37633). A crucial step in DNA methylation involves DNA methyltransferase (Dnmt), which catalyzes the methylation of CpG dinucleotides in genomic DNA.[40] The methylation status of MT promoters is mediated specifically by Dnmt1.[41] Because Dnmt1 contains a predicted miRNA-140-3p target site in its 3′ UTR, with a perfect match to its seed sequences (Fig. 3B), and because the effects of miRNA-140-3p activity were impaired in DDX20-knockdown cells,[25] it was hypothesized that whereas miRNA-140 normally targets and suppresses Dnmt1 protein expression, miRNA-140-3p dysfunction due to DDX20 deficiency results in enhanced Dnmt1 expression, leading to hypermethylation of MT promoters. Consistent with this hypothesis, Dnmt1 expression was increased significantly in DDX20-knockdown cells (Fig. 3C). miRNA-140 precursor overexpression suppressed activity of the Dnmt1 3′ UTR reporter construct, the effect of which was lost when two mutations were introduced into its seed sequences (Fig. 3D). MiRNA-140 precursor overexpression suppressed Dnmt1 protein expression (Fig. 3E). These results indicate that miRNA-140 directly targets Dnmt1 and suppresses its expression in the normal state. Consistently, decreased DDX20, increased Dnmt1, and decreased MT expression were detected together in human clinical HCC samples, as determined via immunohistochemistry (Fig. 3F). By contrast, miRNA-140 precursor-overexpressing Huh7 cells showed increased expression of MTs and reduced NF-κB activity *in vitro* (Supporting Fig. 4A,B). Moreover, the increase in the number of spheres formed from PLC/PRF/5 cells due to DDX20 knockdown was antagonized by treatment with an NF-κB inhibitor or a demethylating agent (Supporting Fig. 5). Taken together, these results suggest that the up-regulated Dnmt1 protein expression caused by functional impairment of miRNA-140-3p due to DDX20 deficiency results in decreased expression of MTs *via* enhanced methylation at the CpG sites in their promoters. This may lead to enhanced NF-κB activity and cellular transformation at least *in vitro*.

MiRNA-140 Is a Liver Tumor Suppressor. To further examine the biological consequences of functional impairment of miRNA-140 due to DDX20 deficiency, we determined the phenotypes of miRNA-140 knockout (miRNA-140$^{-/-}$) mice (Fig. 4A). Similar to the *in vitro* DDX20 knockdown results, Dnmt1 expression was increased and MT levels decreased in the liver tissue of these mice (Fig. 4B). NF-κB–DNA binding activity was enhanced in the livers of miRNA-140$^{-/-}$ mice after tail-vein injection of TNF-α, a crucial cytokine that induces NF-κB activity and hepatocarcinogenesis (Fig. 4C). As was found in MT knockout mice, phosphorylation of p65 at serine 276, which is critical for p65 activation, was significantly increased in the livers of miRNA-140$^{-/-}$ mice after DEN exposure, which induces NF-κB activation and liver tumors[37] (Fig. 4D). Notably, the size and number of liver tumors that developed 8 months after DEN exposure were markedly elevated in miRNA-140$^{-/-}$ mice compared with control mice (Fig. 4E,F). These results indicate that miRNA-140$^{-/-}$ mice are indeed

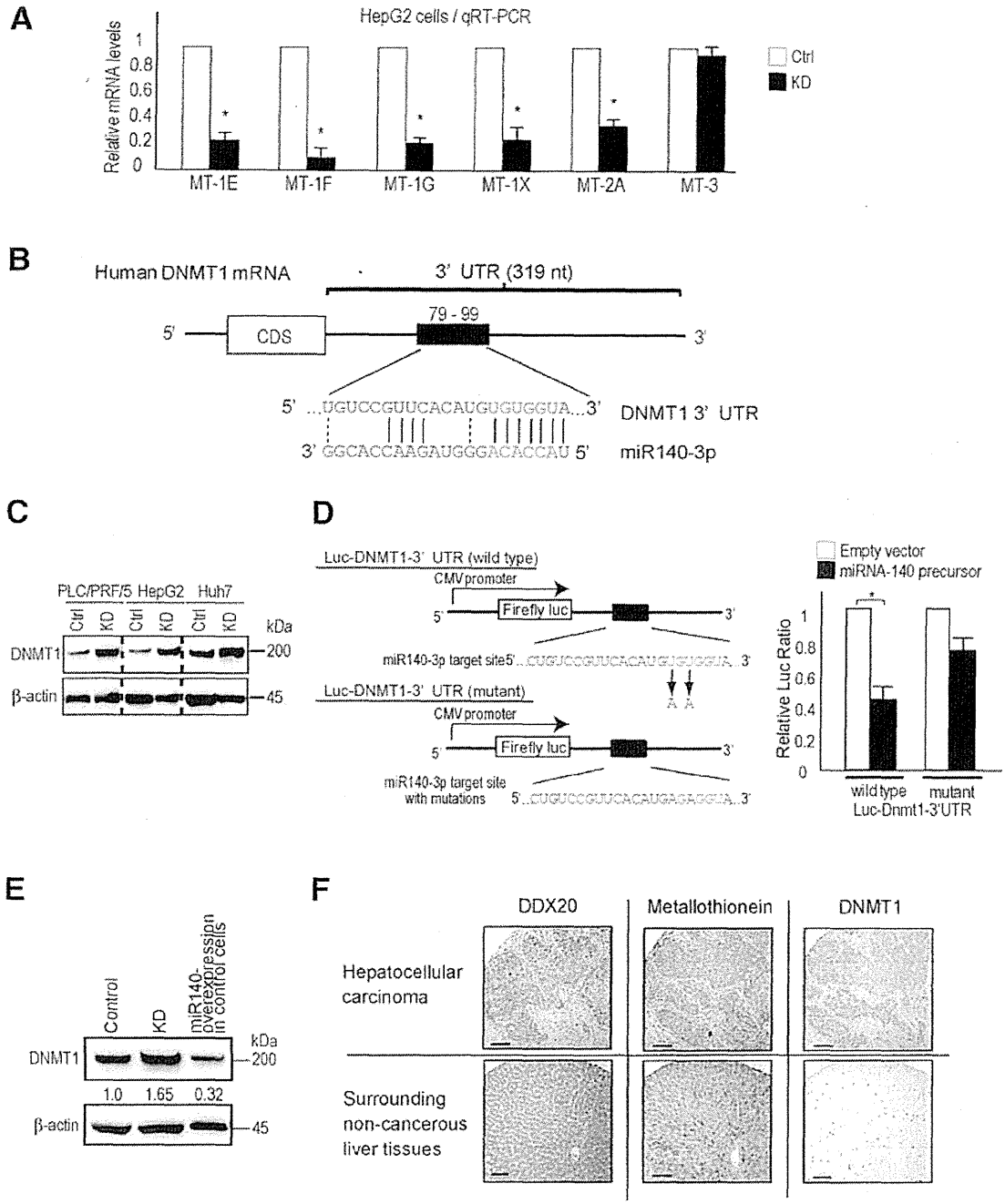

Fig. 3. Targeting of Dnmt1 by miRNA-140-3p and reduced MT expression. (A) The expression levels of MTs were determined using quantitative reverse-transcriptase polymerase chain reaction. The relative expression ratios of the MTs in control (white bars) and DDX20-knockdown (black bars) HepG2 cells were calculated by normalizing control cell values to 1.0. The data represent the mean ± SD of three independent determinations. $*P < 0.05$. (B) Putative miRNA-140-3p target sites in the 3′ UTR of human Dnmt1. Seed sequences are indicated in red. (C) Dnmt1 expression was increased in DDX20-knockdown cells. Ctrl, control cells; KD, DDX20-knockdown cells. (D) Left: Schematic diagrams of wild-type (upper) and mutant (lower) luciferase reporter constructs (Luc-Dnmt1-3′ UTRs) carrying the Dnmt1 3′ UTR region harboring the putative miRNA-140-3p target site. The mutant seed sequence contained two nucleotide substitutions. Right: The Dnmt1 3′ UTR is targeted directly by miRNA-140-3p. Cells were cotransfected with Luc-Dnmt1-3′ UTR (wild-type or mutant) plus either an empty vector (white bars) or a plasmid expressing the miRNA-140 precursor (black bars). Data are the mean ± SD of three independent determinations. (E) Overexpression of miRNA-140 reduces Dnmt1 expression in control cells. Values between the panels indicate Dnmt1 protein levels normalized to those of β-actin. KD, DDX20 knockdown cells. (F) Representative histochemical images showing expression of DDX20, Dnmt1, and MT proteins in HCC (upper three panels) and surrounding tissue (lower panels). Compared with adjacent noncancerous liver tissue, HCCs exhibited decreased DDX20 and MT expression and increased Dnmt1 expression. Note that adjacent sections were stained for each protein. Scale bar, 50 μm.

Table 4. Methylation Levels in CpG Islands of the MT Genes in DDX20-Knockdown HepG2 Cells Compared with Control Cells

Symbol	CpG Island Methylation Ratio	Target ID
MT1E	**1.14**	cg00178359
	1.29	cg06463589
	3.65	cg02512505
	1.02	cg15134649
MT1G	**2.14**	cg16452857
	1.03	cg27367960
	1.00	cg03566142
	0.99	cg07791866
MT1M	**1.16**	cg02132560
	0.98	cg02160530
	1.03	cg04994964
MT1X	**1.24**	cg05596720
	1.05	cg26802333
	1.06	cg09147880
	1.01	cg08872713
MT2A	**2.06**	cg07395075
	0.94	cg20430434

Values were determined using the quantitative Illumina Human Methylation BeadsChip. Boldface values indicate increased methylation levels in DDX20 knockdown cells.

more prone to liver cancer development and suggest that miRNA-140 acts as a liver tumor suppressor, probably by suppressing NF-κB activity, although we cannot completely exclude other molecular mechanisms. Nonetheless, these results also suggest that the impairment of miRNA-140 function due to DDX20 deficiency may lead to hepatocarcinogenesis in humans, as we have observed in miRNA-140$^{-/-}$ mice (Supporting Figs. 6 and 7).

Discussion

Here, we report that miRNA-140$^{-/-}$ mice have increased NF-κB activity and are more prone to HCC development. In addition, we show that DDX20, an miRNP component, is frequently decreased in human HCC tissues. Because DDX20 deficiency preferentially causes impaired miRNA-140 function,[23] the functional impairment of miRNA-140 may result in phenotypes similar to those of miRNA-140$^{-/-}$ mice and may lead to hepatocarcinogenesis. In support of the hypothesis that DDX20 dysfunction is involved in hepatocarcinogenesis, DDX20 is located at 1p21.1-p13.2, a frequently deleted chromosomal region in human HCC,[27] and DDX20 was recently identified as a possible liver tumor suppressor in a functional screen in mice.[27] Although the possibility that intracellular signaling pathways other than miRNA-140 may also be involved in the biological consequences of DDX20 deficiency cannot be denied, we believe that functional impairment of miRNA-140 plays a major role in the phenotypes induced by DDX20 deficiency, based on the phenotypic similarities.

Changes in miRNA expression levels have been reported in various tumors.[7,12,42] However, in this study, we found that reduced expression of an miRNA machinery component might lead to carcinogenesis, at least in part, through functional impairment of miRNAs. Recent studies have shown that components of the RNA interference machinery are associated with the outcome of ovarian cancer patients,[43] and that single-nucleotide polymorphisms in miRNA machinery genes can be used as diagnostic risk markers.[44,45] Therefore, the impairment of miRNA function caused by deregulated miRNA machinery components may also be involved in carcinogenesis.

Our study identified Dnmt1 as a critical target of miRNA-140. The decreased MT expression due to the CpG promoter methylation induced by Dnmt1 resulted in enhanced NF-κB activity. This finding was consistent with the results obtained using MT gene knockout mice, in which enhanced NF-κB activation promoted hepatocarcinogenesis.[37] The decrease in MT expression that results from increased Dnmt1 expression caused by functional impairment of miRNA-140, together with increased NF-κB activation and hepatocarcinogenesis in MT knockout mice,[37] supports the concept that the DDX20/miRNA-140/Dnmt1/MT/NF-κB pathway may play a crucial role in hepatocarcinogenesis. However, we cannot fully exclude the possibility that other intracellular signaling pathways are also involved in the induction of hepatocarcinogenesis by miRNA-140 or DDX20 deficiency, because the precise role of NF-κB in hepatocarcinogenesis has not been clearly defined,[8] although constitutive activation of NF-κB signaling has been frequently detected in human HCCs.[46] The mechanisms by which DDX20 expression is initially decreased and the reason its locus is frequently deleted in HCC remain to be elucidated. However, because DDX20 expression is also regulated by methylation of its CpG promoter,[47] once this pathway is deregulated, decreased DDX20 expression could be maintained by a positive feedback mechanism, even without deletion of its locus.[27]

In conclusion, this study shows that miRNA-140 acts as a liver tumor suppressor. We show that DDX20, an miRNP component, is frequently decreased in human HCC, which may induce hepatocarcinogenesis via impairment of miRNA-140 function. These results suggest the importance of investigations of not only aberrant miRNA expression levels,[12,14,17,48] but also deregulation of miRNP

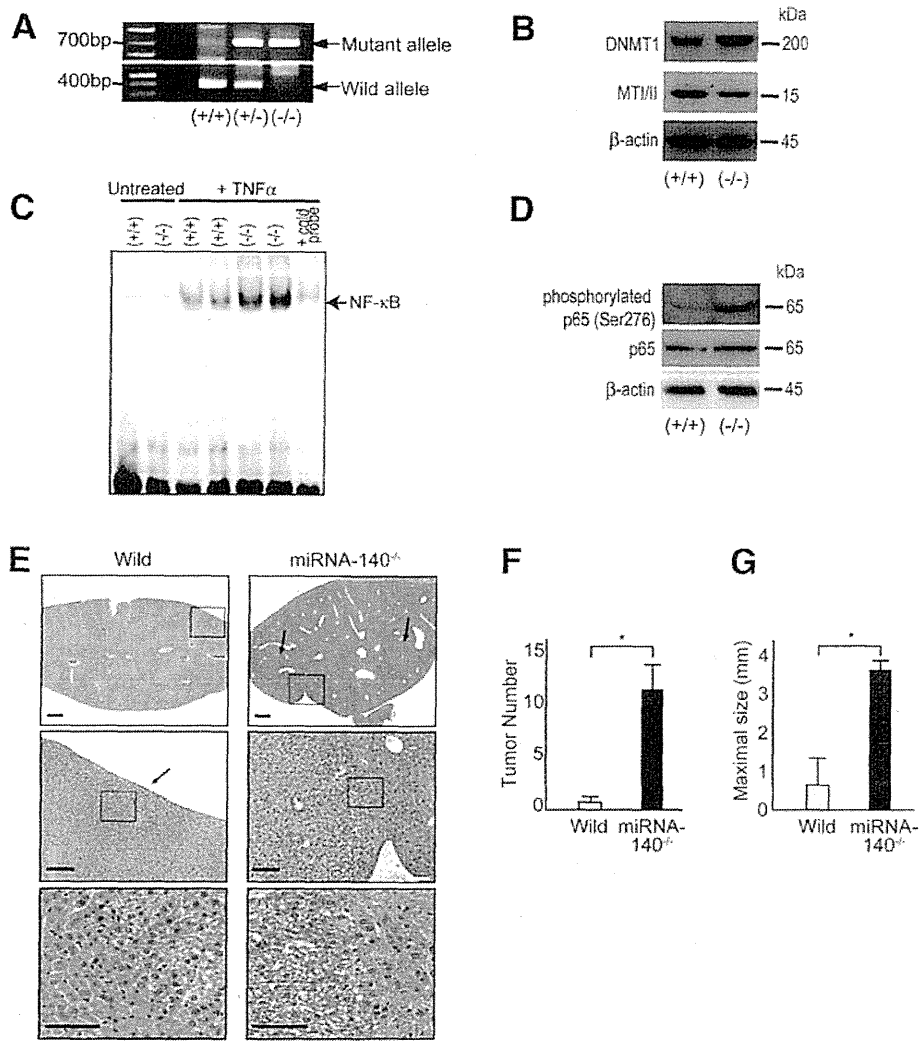

Fig. 4. miRNA-140$^{-/-}$ mice are prone to hepatocarcinogenesis. (A) Representative genotyping of mice with wild-type or mutant alleles. PCR genotyping was performed for miRNA-140 wild-type (419 bp; Wild) and knockout (734 bp; Mutant) alleles. (+/+), wild-type; (+/−), heterozygous; (−/−), knockout. (B) Increased *Dnmt1* expression and decreased MTI/II expression in the liver tissues of miRNA-140$^{-/-}$ mice compared with wild-type mice. Western blotting was performed using antibodies against the indicated proteins. (+/+), wild-type; (−/−), miRNA-140$^{-/-}$. The image shown is representative of four independent experiments. (C) NF-κB–DNA binding was assessed via gel-shift assay using equal amounts of liver nuclear extracts from untreated and TNF-α–injected wild-type and miRNA-140$^{-/-}$ mice. (+/+), wild-type; (−/−), miRNA-140$^{-/-}$. Cold probe was added to TNF-α–injected knockout mouse nuclear extract to test assay specificity. A result representative of four independent experiments is shown. (D) Western blotting for phosphorylated p65 expression in the liver at 32 weeks after DEN treatment in miRNA-140$^{-/-}$ mice compared with wild-type mice. A result representative of four independent experiments is shown. (E) Representative histological images of mouse liver at 32 weeks after DEN treatment. Arrows indicate tumors. Higher-magnification images of the highlighted areas in the upper panels are shown in the lower panels. Scale bar, 500 μm. (F) The number (left panel) and size (right panel) of tumors (five random sections per mouse treated with DEN) are presented as the mean ± SD (wild-type mice, n = 8; miRNA-140$^{-/-}$ mice, n = 8). *$P < 0.05$.

components,[22] with subsequent impairment of miRNA function as molecular pathways and possible therapeutic targets for carcinogenesis and other diseases.

References

1. Parkin D, Bray F, Ferlay J, Pisani P. Global cancer statistics, 2002. CA Cancer J Clin 2005;55:74-108.
2. Block T, Mehta A, Fimmel C, Jordan R. Molecular viral oncology of hepatocellular carcinoma. Oncogene 2003;22:5093-5107.
3. Karin M. Nuclear factor-kappaB in cancer development and progression. Nature 2006;441:431-436.
4. Luedde T, Schwabe RF. NF-κB in the liver—linking injury, fibrosis and hepatocellular carcinoma. Nat Rev Gastroenterol Hepatol 2011;8:108-118.
5. Pikarsky E, Porat R, Stein I, Abramovitch R, Amit S, Kasem S, et al. NF-kappaB functions as a tumour promoter in inflammation-associated cancer. Nature 2004;431:461-466.
6. Liu P, Kimmoun E, Legrand A, Sauvanet A, Degott C, Lardeux B, et al. Activation of NF-kappa B, AP-1 and STAT transcription factors is a frequent and early event in human hepatocellular carcinomas. J Hepatol 2002;37:63-71.

7. Ji J, Shi J, Budhu A, Yu Z, Forgues M, Roessler S, et al. MicroRNA expression, survival, and response to interferon in liver cancer. N Engl J Med 2009;361:1437-1447.
8. Feng GS. Conflicting roles of molecules in hepatocarcinogenesis: paradigm or paradox. Cancer Cell 2012;21:150-154.
9. Bartel DP. MicroRNAs: target recognition and regulatory functions. Cell 2009;136:215-233.
10. Otsuka M, Jing Q, Georgel P, New L, Chen J, Mols J, et al. Hypersusceptibility to vesicular stomatitis virus infection in Dicer1-deficient mice is due to impaired miR24 and miR93 expression. Immunity 2007;27:123-134.
11. Otsuka M, Zheng M, Hayashi M, Lee JD, Yoshino O, Lin S, et al. Impaired microRNA processing causes corpus luteum insufficiency and infertility in mice. J Clin Invest 2008;118:1944-1954.
12. Kojima K, Takata A, Vadnais C, Otsuka M, Yoshikawa T, Akanuma M, et al. MicroRNA122 is a key regulator of α-fetoprotein expression and influences the aggressiveness of hepatocellular carcinoma. Nat Commun 2011;2:338.
13. Chang T-C, Yu D, Lee Y-S, Wentzel EA, Arking DE, West KM, et al. Widespread microRNA repression by Myc contributes to tumorigenesis. Nat Genet 2008;40:43-50.
14. Lu J, Getz G, Miska EA, Alvarez-Saavedra E, Lamb J, Peck D, et al. MicroRNA expression profiles classify human cancers. Nature 2005; 435:834-838.
15. Calin GA, Croce CM. MicroRNA signatures in human cancers. Nat Rev Cancer 2006;6:857-866.
16. Gaur A, Jewell DA, Liang Y, Ridzon D, Moore JH, Chen C, et al. Characterization of microRNA expression levels and their biological correlates in human cancer cell lines. Cancer Res 2007;67:2456-2468.
17. Kumar MS, Lu J, Mercer KL, Golub TR, Jacks T. Impaired microRNA processing enhances cellular transformation and tumorigenesis. Nat Genet 2007;39:673-677.
18. Lambertz I, Nittner D, Mestdagh P, Denecker G, Vandesompele J, Dyer MA, et al. Monoallelic but not biallelic loss of Dicer1 promotes tumorigenesis in vivo. Cell Death Differ 2010;17:633-641.
19. Otsuka M, Takata A, Yoshikawa T, Kojima K, Kishikawa T, Shibata C, et al. Receptor for activated protein kinase C: requirement for efficient microRNA function and reduced expression in hepatocellular carcinoma. PLoS One 2011;6:e24359.
20. Lujambio A, Esteller M. CpG island hypermethylation of tumor suppressor microRNAs in human cancer. Cell Cycle 2007;6:1455-1459.
21. Thomson J, Newman M, Parker J, Morin-Kensicki E, Wright T, Hammond S. Extensive post-transcriptional regulation of microRNAs and its implications for cancer. Genes Dev 2006;20:2202-2207.
22. Melo SA, Ropero S, Moutinho C, Aaltonen LA, Yamamoto H, Calin GA, et al. A TARBP2 mutation in human cancer impairs microRNA processing and DICER1 function. Nat Genet 2009;41:365-370.
23. Takata A, Otsuka M, Yoshikawa T, Kishikawa T, Kudo Y, Goto T, et al. A miRNA machinery component DDX20 controls NF-κB via microRNA-140 function. Biochem Biophys Res Commun 2012;13:564-569.
24. Miyaki S, Sato T, Inoue A, Otsuki S, Ito Y, Yokoyama S, et al. MicroRNA-140 plays dual roles in both cartilage development and homeostasis. Genes Dev 2010;24:1173-1185.
25. Garzon R, Heaphy CE, Havelange V, Fabbri M, Volinia S, Tsao T, et al. MicroRNA 29b functions in acute myeloid leukemia. Blood 2009;114:5331-5341.
26. Mourelatos Z, Dostie J, Paushkin S, Sharma A, Charroux B, Abel L, et al. miRNPs: a novel class of ribonucleoproteins containing numerous microRNAs. Genes Dev 2002;16:720-728.
27. Zender L, Xue W, Zuber J, Semighini C, Krasnitz A, Ma B, et al. An oncogenomics-based in vivo RNAi screen identifies tumor suppressors in liver cancer. Cell 2008;135:852-864.
28. Mouillet J, Yan X, Ou Q, Jin L, Muglia L, Crawford P, et al. DEAD-box protein-103 (DP103, Ddx20) is essential for early embryonic development and modulates ovarian morphology and function. Endocrinology 2008;149:2168-2175.
29. Voss M, Hille A, Barth S, Spurk A, Hennrich F, Holzer D, et al. Functional cooperation of Epstein-Barr virus nuclear antigen 2 and the survival motor neuron protein in transactivation of the viral LMP1 promoter. J Virol 2001;75:11781-11790.
30. Charroux B, Pellizzoni L, Perkinson R, Shevchenko A, Mann M, Dreyfuss G. Gemin3: a novel DEAD box protein that interacts with SMN, the spinal muscular atrophy gene product, and is a component of gems. J Cell Biol 1999;147:1181-1194.
31. Hutvágner G, Zamore P. A microRNA in a multiple-turnover RNAi enzyme complex. Science 2002;297:2056-2060.
32. Takata A, Otsuka M, Kojima K, Yoshikawa T, Kishikawa T, Yoshida H, et al. MicroRNA-22 and microRNA-140 suppress NF-κB activity by regulating the expression of NF-κB coactivators. Biochem Biophys Res Commun 2011;411:826-831.
33. Hu W, Johnson H, Shu H. Tumor necrosis factor-related apoptosis-inducing ligand receptors signal NF-kappaB and JNK activation and apoptosis through distinct pathways. J Biol Chem 1999;274: 30603-30610.
34. Cherian MG, Jayasurya A, Bay BH. Metallothioneins in human tumors and potential roles in carcinogenesis. Mutat Res 2003;533:201-209.
35. Huang GW, Yang LY. Metallothionein expression in hepatocellular carcinoma. World J Gastroenterol 2002;8:650-653.
36. Datta J, Majumder S, Kutay H, Motiwala T, Frankel W, Costa R, et al. Metallothionein expression is suppressed in primary human hepatocellular carcinomas and is mediated through inactivation of CCAAT/enhancer binding protein alpha by phosphatidylinositol 3-kinase signaling cascade. Cancer Res 2007;67:2736-2746.
37. Majumder S, Roy S, Kaffenberger T, Wang B, Costinean S, Frankel W, et al. Loss of metallothionein predisposes mice to diethylnitrosamine-induced hepatocarcinogenesis by activating NF-kappaB target genes. Cancer Res 2010;70:10265-10276.
38. Ghoshal K, Majumder S, Li Z, Dong X, Jacob ST. Suppression of metallothionein gene expression in a rat hepatoma because of promoter-specific DNA methylation. J Biol Chem 2000;275:539-547.
39. Harrington MA, Jones PA, Imagawa M, Karin M. Cytosine methylation does not affect binding of transcription factor Sp1. Proc Natl Acad Sci U S A 1988;85:2066-2070.
40. Li E, Beard C, Jaenisch R. Role for DNA methylation in genomic imprinting. Nature 1993;366:362-365.
41. Majumder S, Kutay H, Datta J, Summers D, Jacob ST, Ghoshal K. Epigenetic regulation of metallothionein-i gene expression: differential regulation of methylated and unmethylated promoters by DNA methyltransferases and methyl CpG binding proteins. J Cell Biochem 2006; 97:1300-1316.
42. Garzon R, Calin G, Croce C. MicroRNAs in cancer. Annu Rev Med 2009;60:167-179.
43. Merritt W, Lin Y, Han L, Kamat A, Spannuth W, Schmandt R, et al. Dicer, Drosha, and outcomes in patients with ovarian cancer. N Engl J Med 2008;359:2641-2650.
44. Horikawa Y, Wood CG, Yang H, Zhao H, Ye Y, Gu J, et al. Single nucleotide polymorphisms of microRNA machinery genes modify the risk of renal cell carcinoma. Clin Cancer Res 2008;14:7956-7962.
45. Yang H, Dinney CP, Ye Y, Zhu Y, Grossman HB, Wu X. Evaluation of genetic variants in microRNA-related genes and risk of bladder cancer. Cancer Res 2008;68:2530-2537.
46. Wu JM, Sheng H, Saxena R, Skill NJ, Bhat-Nakshatri P, Yu M, et al. NF-kappaB inhibition in human hepatocellular carcinoma and its potential as adjunct to sorafenib based therapy. Cancer Lett 2009;278: 145-155.
47. Gebhard C, Schwarzfischer L, Pham T, Andreesen R, Mackensen A, Rehli M. Rapid and sensitive detection of CpG-methylation using methyl-binding (MB)-PCR. Nucleic Acids Res 2006;34:e82.
48. Martello G, Rosato A, Ferrari F, Manfrin A, Cordenonsi M, Dupont S, et al. A microRNA targeting dicer for metastasis control. Cell 2010; 141:1195-1207.

Case Reports in

Case Rep Gastroenterol 2012;6:784–789
DOI: 10.1159/000346462

Published online:
December 22, 2012

© 2012 S. Karger AG, Basel
ISSN 1662–0631
www.karger.com/crg

IGF-II Producing Hepatocellular Carcinoma Treated with Sorafenib: Metabolic Complications and a Foresight to Molecular Targeting Therapy to the IGF Signal

Kazuya Okushin[a] Yoshinari Asaoka[a] Izumi Fukuda[b]
Naoto Fujiwara[a] Tatsuya Minami[a] Masaya Sato[a]
Shintaro Mikami[a] Koji Uchino[a] Kenichiro Enooku[a]
Yuji Kondo[a] Ryosuke Tateishi[a] Tadashi Goto[a]
Shuichiro Shiina[a] Haruhiko Yoshida[a] Kazuhiko Koike[a]

[a]Department of Gastroenterology, Graduate School of Medicine, The University of Tokyo, and [b]Department of Medicine II, Tokyo Women's Medical University, Tokyo, Japan

Key Words
IGF-II · Hepatocellular carcinoma · Sorafenib · Metabolic complications · Molecular targeting therapy · IGF signal · Hypoglycemia

Abstract
Hypoglycemia is a rare paraneoplastic manifestation of patients with neoplasms. Hypoglycemia can be induced by several causes, including an aberrant increase of hypoglycemic agents and adrenal insufficiency. Sorafenib is the first agent to demonstrate a survival benefit in the treatment of advanced hepatocellular carcinoma (HCC). This small molecule inhibits serine/threonine kinase RAF in tumor cells and tyrosine kinases VEGFR/PDGFR in tumor vasculature and decreases tumor growth and angiogenesis. In this paper, we report a case of HCC who was treated with sorafenib and showed severe hypoglycemia. This hypoglycemia might be induced by two causes, both adrenal insufficiency as an adverse effect of sorafenib and activation of the insulin-like growth factor (IGF) signal by excessive secretion of incompletely processed precursors of IGF-II. Although the IGF signal is suggested to be involved in aberrant growth of HCC in some cases, there is no other report showing the influence of sorafenib on HCC with active IGF signal. Unfortunately, the effect of sorafenib was limited in the present case. However, emerging drugs that directly inhibit the IGF signal can be expected to be highly effective in the treatment of HCC with hypoglycemia.

Kazuya Okushin

Department of Gastroenterology, Graduate School of Medicine
The University of Tokyo, 7-3-1 Hongo, Bunkyo-ku
Tokyo 113-8655 (Japan)
E-Mail koxin-tky@umin.org

Case Reports in | Case Rep Gastroenterol 2012;6:784–789 DOI: 10.1159/000346462 | Published online: December 22, 2012 | © 2012 S. Karger AG, Basel ISSN 1662–0631 www.karger.com/crg

Introduction

Hypoglycemia is a rare but well-known paraneoplastic manifestation of patients with neoplasms, including hepatocellular carcinoma (HCC), which is referred to as non-islet cell tumor-induced hypoglycemia (NICTH) [1]. Excessive secretion of incompletely processed precursors of insulin-like growth factor-II (termed the 'big' IGF-II) has been suggested to cause NICTH. The IGF signal is involved in both glucose metabolism and cellular proliferation [2]. The 'big' IGF-II excessively stimulates both IGF-I and the insulin receptor, inducing hypoglycemia and tumor growth. In the era of molecular-targeted therapy, agents targeting the IGF signal are being developed to treat lung and pancreatic cancers [3]. Although this signal is suggested to be involved in aberrant growth of HCC [4], clinical trials using these agents against HCC have been initiated only recently.

Sorafenib is the first agent to demonstrate a survival benefit in the treatment of advanced HCC [5]. This small molecule inhibits serine/threonine kinase RAF in tumor cells and tyrosine kinases vascular endothelial growth factor receptor (VEGFR)/platelet-derived growth factor receptor (PDGFR) in the tumor vasculature, decreasing tumor growth and angiogenesis.

In this paper, we report a case of HCC that showed severe hypoglycemia and was treated with sorafenib. Since RAF is one of the downstream components of the IGF signal, sorafenib may be effective against tumors with an activated IGF signal. Although the effect was limited in the present case, emerging drugs that directly inhibit the IGF signal can be expected to be highly effective in the treatment of HCC with NICTH.

Case Report

A 77-year-old male patient with HCC was referred to the authors' hospital. As he had no previous episodes of liver disorders, no imaging procedures had been performed. In February 2010, he was first admitted to another hospital due to bleeding gastric ulcers induced by non-steroidal anti-inflammatory drugs. During hospitalization, an abdominal CT scan showed multiple liver tumors and multiple lung nodules (fig. 1a, b). Based on elevated serum AFP (897 ng/ml) and typical CT scan images as HCC, he was diagnosed as advanced HCC and referred to our hospital in March 2010.

Administration of sorafenib was initiated at a dosage of 800 mg b.i.d. On day 7, pleural effusion was detected and his serum potassium concentration was elevated to 5.5 mEq/l. His general condition declined and he was unable to stand by day 11. On day 14, he was hospitalized because of hyperpotassemia (6.7 mEq/l) and hypoglycemia (27 mg/dl). Hyperpotassemia improved by the administration of an intravenous drip infusion of glucose and furosemide, but hypoglycemia continued at a level of 40 mg/dl. Although the basal levels of adrenal hormones were normal, ACTH and cortisol did not increase at the time of hypoglycemia. This suggested that the relative adrenal insufficiency exerted some influence on the hypoglycemia. We started to administer a short-acting corticosteroid (hydrocortone), and the blood glucose level increased rapidly to around 150 mg/dl.

However, several days later, the patient's morning fasting blood glucose level decreased to around 20 mg/dl. We administrated a longer-acting corticosteroid and the patient also began to have late evening snacks. Although a sufficient amount of cortisol (prednisolone 10 mg/day) was administered, his hypoglycemia continued. We suspected that other factors were involved in the hypoglycemia, but the serum levels of insulin and IGF-I were lower than the normal limits. We assayed the patient's serum using immunoblotting with an anti-IGF-II antibody. The 'big' IGF-II was detected in the serum (fig. 2, lane 2) similarly to the serum of a patient with NICTH (lane 4). Only mature IGF-II was detected in the serum of the normal control (lane 3). Lane 1 was recombinant IGF-II.

Case Reports in | Case Rep Gastroenterol 2012;6:784–789 DOI: 10.1159/000346462 | Published online: December 22, 2012 | © 2012 S. Karger AG, Basel ISSN 1662–0631 www.karger.com/crg

By day 14 of sorafenib administration, though the number of lung metastases had increased (fig. 1d), the size of the liver tumors had not changed (fig. 1c) and the tumor marker levels had decreased (AFP from 4,112 to 2,381 ng/ml and PIVKA-II from 4,645 to 952 mAU/ml) (fig. 3). We concluded that sorafenib was effective. The dose of sorafenib was decreased to half (400 mg b.i.d.), and the patient was discharged. Ten days later, he was hospitalized because of unconsciousness caused by hypoglycemia. Though the hypoglycemia improved with treatments, sadly the patient died 6 days later of respiratory failure due to advanced lung metastases.

Discussion

We treated a case of IGF-II producing HCC with sorafenib. Several previous reports have shown NICTH as a rare paraneoplastic manifestation of advanced HCC with a poor prognosis [6]. As far as we are aware, there are no reports describing HCC with NICTH treated with this novel molecular targeted agent, sorafenib. The present case showed interesting endocrine abnormalities such as hypoglycemia and hyperpotassemia due to relative adrenal insufficiency. The possibility that sorafenib suppressed adrenal function must be considered, since there were no other factors known to affect adrenal function such as metastasis to the adrenal glands. No reports have been identified that describe adrenal insufficiency due to sorafenib, while the drug is reported to affect thyroid functions. The possibility that sorafenib played a role in adrenal insufficiency is also supported by the fact that there are some reports of adrenal dysfunction caused by a similar molecular agent, sunitinib, targeting VEGFR/PDGFR [7].

The IGF signal is related to cell proliferation and tumor growth of HCC through the IGF-I receptor [4]. Kaseb et al. [8] reported that lower plasma IGF-I levels are correlated with advanced HCC and poor overall survival. Reactivation of IGF-II, including the 'big' IGF-II, is one of the most frequent mechanisms of IGF signal activation in HCC. Expression of IGF-I may be suppressed by a negative feedback of IGF-II overexpression, resulting in lower plasma IGF-I levels.

The 'big' IGF-II is suggested to induce hypoglycemia through IGF-I and the insulin receptor. Usually, hypoglycemia due to the 'big' IGF-II is not controllable with continuous infusion of glucose. Reduction of tumor volume by surgical operation [9], transarterial chemoembolization or systemic chemotherapy [1] is sometimes effective. Palliative treatments, including administration of hyperglycemic hormones such as corticosteroids and growth hormones, are performed, but the effects are transient and limited.

When the IGF-I receptor is stimulated, the downstream signaling pathways, including PI3K-AKT-TOR and RAF-MEK-ERK, are activated [2]. Sorafenib inhibits the activation of RAF. However, the efficacy of sorafenib was limited in the present case (fig. 3). Several drugs that target the IGF signal are under development [3]. Such drugs directly inhibit intracellular kinase activities or block the binding of IGF to the receptors. We suggest that these agents will likely be effective in NICTH cases. In particular, use of antibodies against IGF-II will probably be selective and safe in such cases.

Case Reports in

Case Rep Gastroenterol 2012;6:784–789
DOI: 10.1159/000346462

Published online:
December 22, 2012

ISSN 1662–0631
www.karger.com/crg

Acknowledgements

This work was supported in part by Health Sciences Research Grants of The Ministry of Health, Labor and Welfare of Japan (Research on Hepatitis).

Disclosure Statement

The authors have no competing interests to disclose.

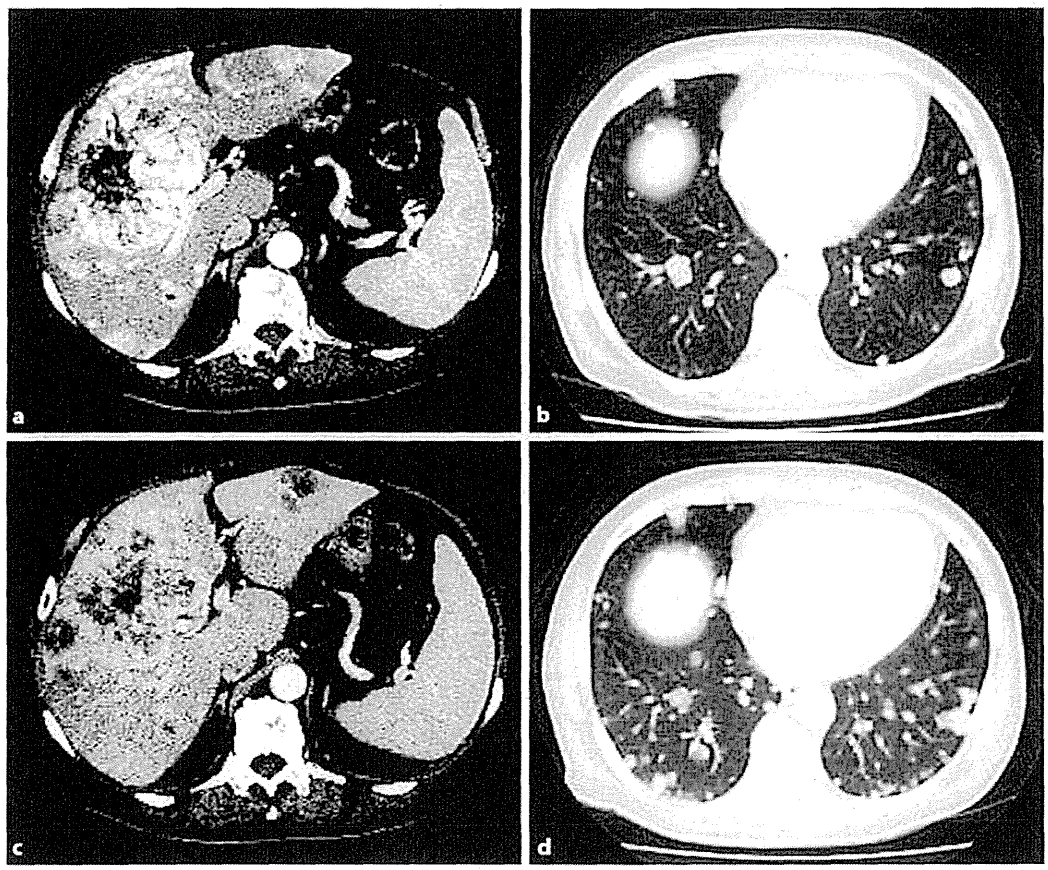

Fig. 1. CT scan images before and after the administration of sorafenib. **a**, **b** Images before therapy. **c**, **d** Images after therapy. By the administration of sorafenib, the size of the liver tumors had not changed (**a** to **c**), but the number of lung metastases had increased (**b** to **d**).

Case Reports in | Case Rep Gastroenterol 2012;6:784–789 DOI: 10.1159/000346462 | Published online: December 22, 2012 | © 2012 S. Karger AG, Basel ISSN 1662–0631 www.karger.com/crg

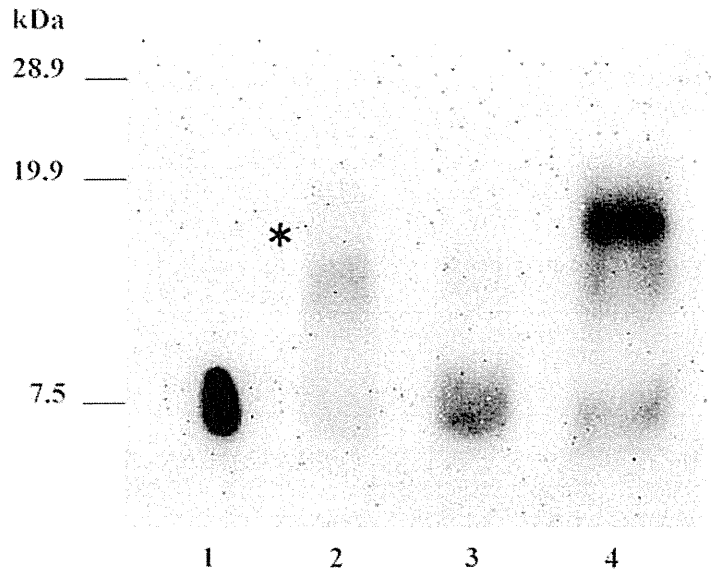

Fig. 2. Immunoblotting images of the patient's serum with an anti-IGF-II antibody. The 'big' IGF-II was detected in the patient's serum (lane 2, asterisk) similarly to the serum of a patient with NICTH (lane 4). Only mature IGF-II was detected in the serum of the normal control (lane 3). Lane 1 is recombinant IGF-II.

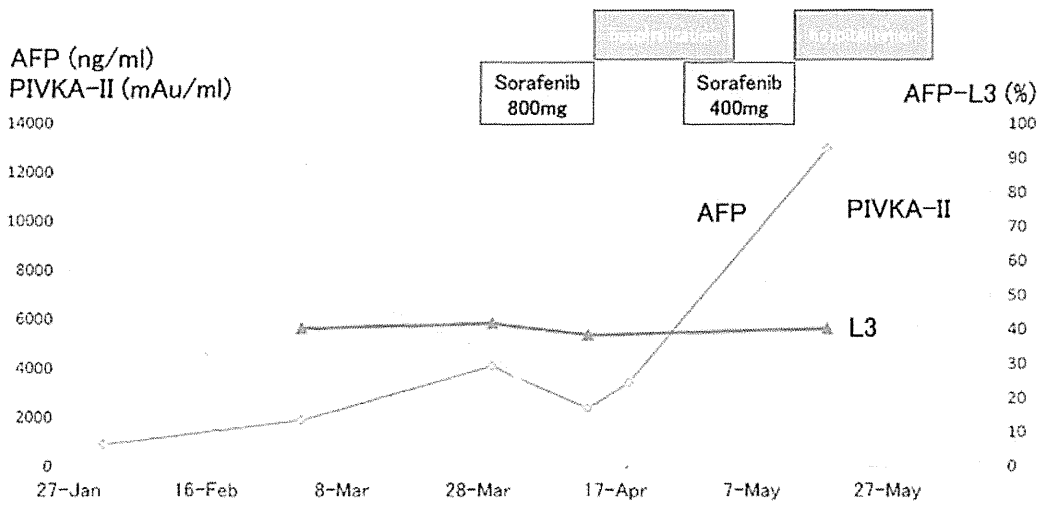

Fig. 3. Changes in the tumor marker levels before and after the administration of sorafenib. By day 14 of sorafenib administration, the tumor marker levels had decreased (AFP from 4,112 to 2,381 ng/ml and PIVKA-II from 4,645 to 952 mAU/ml). However, the effects were transient and the tumor marker levels increased again in spite of the administration of sorafenib.

Case Reports in | Case Rep Gastroenterol 2012;6:784–789 DOI: 10.1159/000346462 | Published online: December 22, 2012 | © 2012 S. Karger AG, Basel ISSN 1662–0631 www.karger.com/crg

References

1 de Groot JW, Rikhof B, Van Doorn J, Bilo HJ, Alleman MA, Honkoop AH, Van Der Graaf WT: Non-islet cell tumour-induced hypoglycaemia: a review of the literature including two new cases. Endocr Relat Cancer 2007;14:979–993.

2 Pollak M: Insulin, insulin-like growth factors and neoplasia. Best Pract Res Clin Endocrinol Metab 2008;22:625–638.

3 Gualberto A, Pollak M: Emerging role of insulin-like growth factor receptor inhibitors in oncology: early clinical trial results and future directions. Oncogene 2009;28:3009–3021.

4 Scharf JG, Dombrowski F, Ramadori G: The IGF axis and hepatocarcinogenesis. Mol Pathol 2001;54: 138–144.

5 Llovet JM, Ricci S, Mazzaferro V, Hilgard P, Gane E, Blanc JF, de Oliveira AC, Santoro A, Raoul JL, Forner A, Schwartz M, Porta C, Zeuzem S, Bolondi L, Greten TF, Galle PR, Seitz JF, Borbath I, Haussinger D, Giannaris T, Shan M, Moscovici M, Voliotis D, Bruix J: Sorafenib in advanced hepatocellular carcinoma. N Engl J Med 2008;359:378–390.

6 Fukuda I, Hizuka N, Ishikawa Y, Yasumoto K, Murakami Y, Sata A, Morita J, Kurimoto M, Okubo Y, Takano K: Clinical features of insulin-like growth factor-II producing non-islet-cell tumor hypoglycemia. Growth Horm IGF Res 2006;16:211–216.

7 Rock EP, Goodman V, Jiang JX, Mahjoob K, Verbois SL, Morse D, Dagher R, Justice R, Pazdur R: Food and Drug Administration drug approval summary: Sunitinib malate for the treatment of gastrointestinal stromal tumor and advanced renal cell carcinoma. Oncologist 2007;12:107–113.

8 Kaseb AO, Morris JS, Hassan MM, Siddiqui AM, Lin E, Xiao L, Abdalla EK, Vauthey JN, Aloia TA, Krishnan S, Abbruzzese JL: Clinical and prognostic implications of plasma insulin-like growth factor-1 and vascular endothelial growth factor in patients with hepatocellular carcinoma. J Clin Oncol 2011;29: 3892–3899.

9 Renard E, Langbour-Remy C, Klein M, Le Bouc Y, Weryha G, Cuny T: Severe hypoglycemia with 'Big'-IGF-2 oversecretion by a giant phyllode tumor of the breast: a rare case of non-islet cell tumor-induced hypoglycemia (NICTH). Ann Endocrinol 2012;73:488–491.

J Infect Chemother (2012) 18:883–890
DOI 10.1007/s10156-012-0433-4

ORIGINAL ARTICLE

Chronic hepatitis B in patients coinfected with human immunodeficiency virus in Japan: a retrospective multicenter analysis

Shintaro Yanagimoto · Hiroshi Yotsuyanagi · Yoshimi Kikuchi · Kunihisa Tsukada · Michio Kato · Junki Takamatsu · Shuhei Hige · Kazuaki Chayama · Kyoji Moriya · Kazuhiko Koike

Received: 14 January 2012 / Accepted: 10 May 2012 / Published online: 4 July 2012

Abstract A nationwide survey in Japan revealed that about 6 % of human immunodeficiency virus (HIV)-positive patients are coinfected with hepatitis B virus (HBV). To further analyze the features of liver disease in HIV/HBV-coinfected patients, we analyzed 252 patients from six hospitals in the HIV/AIDS (acquired immunodeficiency syndrome) Network of Japan. The mean age was 39.5 years, and the proportion of male patients was very high (243 of 252; 96 %). The main transmission route was male homosexual contact (186 of 252; 74 %), followed by heterosexual contact. The HBV genotype was determined in 77 patients. Among them, genotype A HBV was the most frequent (58 of 77; 75 %) and was detected almost exclusively in homosexual patients. Acute hepatitis B was documented in 21 patients (8 %). Three of the 252 HIV/HBV-coinfected patients developed advanced liver disease with the complication of ascites, hepatic encephalopathy, or hepatocellular carcinoma. A comparison between patients not treated and those treated with antiretroviral drugs including anti-HBV drugs revealed that the baseline liver function was worse in treated patients. However, the serum albumin levels and platelet counts in both groups increased after treatment and were similar. Liver disease-associated death was not observed. Here, we characterize the clinical features of liver disease in HIV/HBV-coinfected patients in Japan for the first time. The findings suggest that antiretroviral therapy with anti-HBV drugs may retard the progression of a liver disease and prevent liver disease-associated death in such patients.

Keywords Acquired immunodeficiency syndrome · Chronic liver disease · HBV DNA · Genotype

S. Yanagimoto · H. Yotsuyanagi (✉) · K. Moriya · K. Koike
Department of Internal Medicine, Graduate School of Medicine, University of Tokyo, 7-3-1 Hongo, Bunkyo-ku, Tokyo 113-8655, Japan
e-mail: hyotsu-tky@umin.ac.jp

Y. Kikuchi · K. Tsukada
AIDS Clinical Center, International Medical Center of Japan, Tokyo, Japan

M. Kato
Department of Gastroenterology, Osaka National Hospital, Osaka, Japan

J. Takamatsu
Division of Transfusion Medicine, Nagoya University Hospital, Nagoya, Japan

S. Hige
Department of Gastroenterology and Hematology, Hokkaido University Graduate School of Medicine, Sapporo, Japan

K. Chayama
Department of Medicine and Molecular Science, Graduate School of Biomedical Sciences, Hiroshima University, Hiroshima, Japan

Introduction

The number of human immunodeficiency virus (HIV)-positive patients is growing in Japan [1]. Although combination therapy with antiretroviral agents has made HIV infection itself somewhat controllable in many cases since its introduction in 1996, and mortality from opportunistic infection has decreased, existing comorbidities are the focus of current patient care. In fact, more than 50 % of deaths in HIV-1-infected patients are not related to acquired immunodeficiency syndrome (AIDS); the mortality from liver disease is second only to AIDS-related mortality [2]. Risk factors related to significant liver

diseases among HIV-positive patients include a diagnosis of viral hepatitis [3], nonalcoholic fatty liver disease [4], and excessive alcohol consumption [5]. Among these factors, hepatitis B and hepatitis C are of particular importance because they can often lead to life-threatening diseases such as cirrhosis and hepatocellular carcinoma by themselves.

The estimated prevalence of chronic hepatitis B virus (HBV) infection in Japan is less than 1 %, or 0.9 million carriers [6]. However, about 6 % of HIV-positive patients are coinfected with HBV [7]; this coinfection rate is more than six times higher than that in the non-HIV population. In the United States, the HIV/HBV coinfection rate is reported to be in the range of 6–14 % [8–10].

Several issues make the management of HIV/HBV coinfection complicated. HBV infection tends to be persistent in HIV-positive patients [9, 11, 12]. Chronic HBV infection may lead to hepatitis, cirrhosis, or hepatocellular carcinoma. The progression of a liver disease associated with chronic HBV infection is more rapid in HIV/HBV-coinfected patients than in HBV-monoinfected patients [13].

Combination regimens of antiretroviral therapy (ART) for coinfected patients should be carefully determined. Initial combination regimens of ART for HIV/hepatitis C virus (HCV)-coinfected patients are basically the same as those for HIV patients without HCV infection. However, because some nucleoside reverse transcriptase inhibitors (NRTIs) used in HIV treatment have activity against HBV, and some NRTIs mainly used in HBV treatment have partial activity against HIV [14], careful choice of treatment agents is necessary in HIV/HBV coinfection. Abrupt discontinuation of NRTIs that are active against HBV may aggravate viral hepatitis. Administration of entecavir, which has a weak activity against HIV, to HIV/HBV-coinfected patients without simultaneous effective HIV treatment may cause the accumulation of drug-resistant HIV strains [15–17]. In such cases, drug resistance of HBV may occur as well [18].

Drug-induced liver injury following ART is another concern. HIV/HBV-coinfected patients show an increase in transaminase level at a higher rate [19, 20]. However, it is often unclear whether this increase is caused by drug hepatotoxicity because the treatment of HIV infection causes immune reconstruction in patients, which alone could contribute to the transaminase level increase in viral hepatitis.

The objective of this study is to clarify the clinical features of HIV/HBV coinfection in Japan and to clarify the impact of ART on liver function among HIV/HBV-coinfected patients. The estimated prevalence of chronic HBV infection among the general population in Japan is decreasing yearly, but it remains much higher than that in the United States [21], where universal hepatitis B vaccination is introduced. Thus, the detailed analysis of HIV/HBV coinfection in Japan is of particular importance.

Patients and methods

We have conducted a multicenter retrospective study based on the data from a nationwide survey in 2006 conducted by sending questionnaires to 372 member hospitals of the HIV/AIDS network of Japan as of January 2006, and part of the results was reported earlier [7]. Following the survey, 6 of the 207 hospitals that responded to the survey—Hokkaido University Hospital (Hokkaido, Japan), University of Tokyo Hospital (Tokyo, Japan), Nagoya University Hospital (Aichi, Japan), International Medical Center of Japan (currently, National Center for Global Health and Medicine, Tokyo, Japan), Osaka National Hospital (Osaka, Japan), and Hiroshima University Hospital (Hiroshima, Japan)—were chosen for further studies because more than two-thirds of the HIV/HBV-coinfected patients identified in the survey went to these hospitals, and because both HIV experts and hepatologists were following up those patients there.

The questionnaire sent to the hospitals included items regarding the number of patients who visited the hospitals at least once between January and December in 2006 as follows: (1) the number of HIV-positive patients; (2) the number of hepatitis B surface antigen (HBsAg)-positive patients among (1); (3) the number of patients among (2) who were determined at least once to have a serum alanine aminotransferase (ALT) level higher than 100 IU/l; (4) the number of HIV-positive patients who contracted HIV from blood products; (5) the number of HBsAg-positive patients among (4); (6) the number of patients among (5) who were determined at least once to have a serum ALT level higher than 100 IU/l; (7) the number of HIV-positive patients whose presumed transmission route is through homosexual contact; (8) the number of HBsAg-positive patients among (7); (9) the number of patients among (8) who were determined at least once to have a serum ALT level higher than 100 IU/l; (10) the number of HIV-positive patients who presumably contracted HIV through injection drug use; (11) the number of HBsAg-positive patients among (10); (12) the number of patients among (11) who were determined at least once to have a serum ALT level higher than 100 IU/l; (13) the number of HIV-positive patients whose transmission routes were classified as "others"; (14) the number of HBsAg-positive patients among (13); and (15) the number of patients among (15) who were determined at least once to have a serum ALT level higher than 100 IU/l.

We defined confirmed HIV infection with positivity for serum HBsAg as the criterion for HIV/HBV coinfection.